



**HAL**  
open science

# Exploitation of the far-offshore wind energy resource by fleets of energy ships. Part A. Energy ship design and performance

Aurélien Babarit, Gaël Clodic, Simon Delvoye, Jean-Christophe Gilloteaux

## ► To cite this version:

Aurélien Babarit, Gaël Clodic, Simon Delvoye, Jean-Christophe Gilloteaux. Exploitation of the far-offshore wind energy resource by fleets of energy ships. Part A. Energy ship design and performance. Wind Energy Science, 2020, 10.5194/wes-2019-100 . hal-02870631

**HAL Id: hal-02870631**

**<https://hal.science/hal-02870631>**

Submitted on 16 Jun 2020

**HAL** is a multi-disciplinary open access archive for the deposit and dissemination of scientific research documents, whether they are published or not. The documents may come from teaching and research institutions in France or abroad, or from public or private research centers.

L'archive ouverte pluridisciplinaire **HAL**, est destinée au dépôt et à la diffusion de documents scientifiques de niveau recherche, publiés ou non, émanant des établissements d'enseignement et de recherche français ou étrangers, des laboratoires publics ou privés.

# Exploitation of the far-offshore wind energy resource by fleets of energy ships. Part A. Energy ship design and performance

Aurélien Babarit<sup>1</sup>, Gaël Clodic<sup>1</sup>, Simon Delvoe, Jean-Christophe Gilloteaux<sup>1</sup>

<sup>1</sup>LHEEA, Ecole Centrale de Nantes - CNRS, Nantes, 44300, France

5 *Correspondence to:* Aurélien Babarit (aurelien.babarit@ec-nantes.fr)

**Abstract.** This paper deals with a new concept for the conversion of far-offshore wind energy into sustainable fuel. It relies on autonomously sailing energy ships and manned support tankers. Energy ships are wind-propelled. They generate electricity using water turbines attached underneath their hull. Since energy ships are not grid-connected, they include onboard power-to-X plants for storage of the produced energy. In the present work, the energy vector is methanol.

10 The aim of the paper is to propose an energy ship design and to provide an estimate for its energy performance as function of the wind conditions. The energy performance assessment is based on a numerical model which is described in the paper. Results show that the wind energy-to-methanol (chemical energy) conversion efficiency is 24% and that such energy ship deployed in the North Atlantic Ocean could produce approximately 5 GWh per annum of chemical energy (900 tonnes of methanol per annum).

## 15 1 Introduction

To date, fuels such as oil, natural gas and coal account for approximately 80% of primary energy consumption globally (BP, 2018). Although this share is expected to decrease with the development of renewable power generation and the electrification of the global economy, some sectors may be difficult to electrify (e.g. aviation, freight). Therefore, if a global temperature change of less than 2°C—as set out in the Paris agreement (UNFCCC, 2015) — is to be achieved, there is a  
20 critical need to develop low-carbon alternatives to fossil fuels.

A promising option is the production of sustainable fuel from renewable power generation sources, through power-to-gas and power-to-liquid processes (PtX processes) (Gotz et al., 2016). Several demonstration projects have shown the technical feasibility of such approaches, e.g. Jupiter 1000 in France, BMWi in Germany, SOLETAIR in Finland (Vazquez et al., 2018), George Olah PtL plant in Iceland (Marlin et al., 2018), among others. However, the main challenge faced by PtX  
25 products from renewable energy-based plants is cost competitiveness. Key economic drivers are the cost of input electricity to the PtX plant and the PtX plant capacity factor (Fasihi et al., 2016; Ioannou and Brennan, 2019). Unfortunately, there is currently no commercial renewable power generation technology which can combine the large-scale deployment potential, low cost of generated electricity and high capacity factor which are required for the large-scale synthesis of competitive sustainable fuel from PtX processes.

30 The conversion of far-offshore wind energy resource into sustainable fuel may address this challenge. Indeed, the deployment potential is enormous as over 70% of the surface of our planet is covered by oceans. Moreover, high capacity factors could be achieved as the wind energy resource is the strongest and the steadiest in the open ocean (Liu et al., 2008). In this respect, it has already been shown that capacity factors greater than 80% could be obtained for floating grid-connected stationary offshore wind turbines deployed in the far-offshore (Dupont et al., 2018; Abd-Jamil et al., 2019).  
 35 However, it is not possible to deploy such turbines because grid-connection cost, moorings and installation cost, and maintenance increase dramatically as distance to shore and water depth increase (Offshore wind programme board, 2016). Therefore, alternative concepts are required.

The possibilities include the sailing wind turbine concept (Vidal, 1983) and the energy ship concept (Platzer and Sarigul-Klijn, 2009). The sailing wind turbine concept consists in a floating barge equipped with a wind turbine and propellers. It is  
 40 neither moored nor grid-connected. The position is controlled via the action of the propellers. The energy ship is a ship propelled by the wind and which generates electricity by means of a water turbine attached underneath its hull. In both concepts, the generated electricity is stored on-board, which can be achieved by its conversion into fuel using an onboard power-to-gas (e.g. hydrogen) or power-to-liquid plant (e.g. methanol).

This study focuses on the energy ship concept. Despite the fact that the initial idea was patented as early as 1982 (Salomon,  
 45 1982), it did not receive much attention until the end of the first decade of the 2000s. Thus, there has been only a limited number of energy ships' proposals to date. They include (Meller, 2006; Gizarra, 2007; Kim and Park, 2010; Babarit and Gilloteaux, 2017; and Ouchi and Henzie, 2017). They implement quite diverse technologies for the subsystems (sails, water turbines, hull shapes, etc.) as can be seen in Fig. 1.

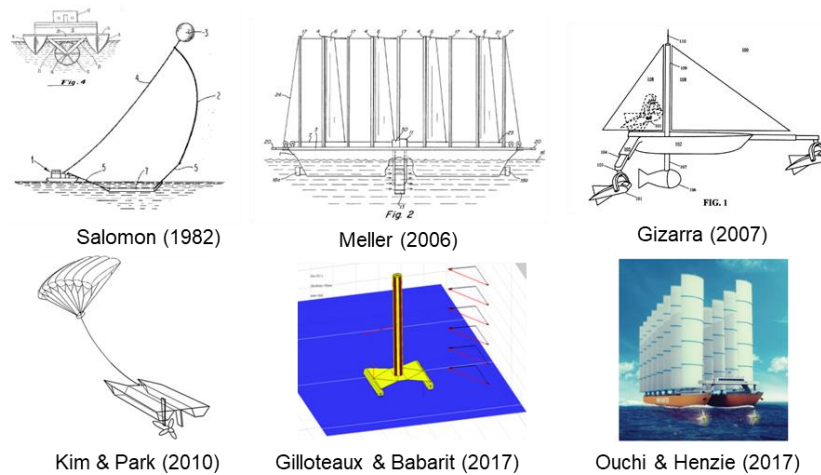


**Figure 1 Pictures of technology proposals of energy ships.**

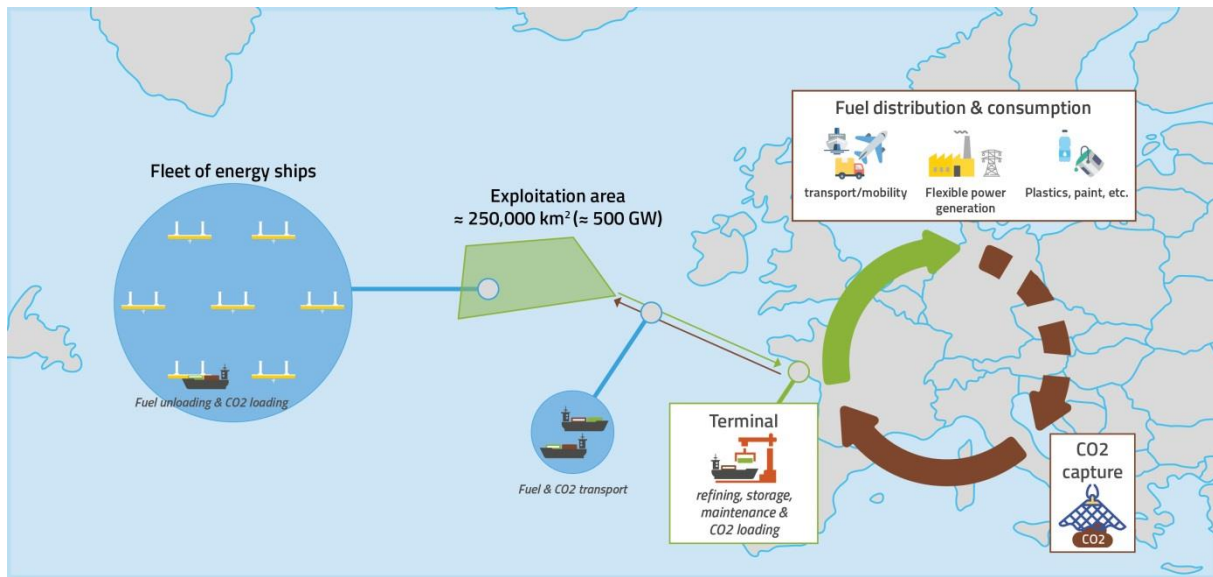
50 In 2009, Platzer & Sarigul-Klijn were the first to describe this concept in a scientific publication (Platzer and Sarigul-Klijn, 2009), proposing it as a way to increase hydrokinetic energy sources for water turbines. The following year, Kim & Park presented a concept that included kite sails flown at high altitude (1,500m) for wind propulsion, a catamaran for the hull, and

hydrogen or methanol for the energy vector (Kim and Park, 2010). Using a velocity prediction program (VPP), they showed  
55 that MW-scale power production is possible with ships of dimensions similar to that of typical commercial ships. They also  
showed that the energy potential is considerable, and could cover several times the global energy demand. In the following  
years, Platzer et al. showed that MW-scale power production is also possible with ships fitted with conventional sails  
exploiting low altitude wind energy (Platzer et al., 2013; Platzer et al., 2014).

With respect to energy storage aboard energy ships, the use of batteries has been proposed by Platzer & Sarigul-Klijn in  
60 (Platzer and Sarigul-Klijn, 2015). However, high gravimetric and high volumetric energy densities are key requirements for  
high performance energy ships in order to minimize water resistance (Pelz et al., 2016; Gilloteaux and Babarit, 2017). Thus,  
the conversion of the produced electricity into fuel through PtG or PtL processes is the most promising solution (Chen et al.,  
2009), which is why hydrogen produced from water electrolysis has been chosen for the energy vector in most energy ship  
proposals (Platzer and Sarigul-Klijn, 2009; Salomon, 1982; Kim and Park, 2010; Gilloteaux and Babarit, 2017; Ouchi and  
65 Henzie, 2017)[24].

However, low volumetric energy density at ambient temperature and pressure conditions is a well-known challenge for  
hydrogen storage and transportation. In (Babarit et al., 2018), the energy cost and economic cost of hydrogen storage and  
transportation was estimated for far-offshore and land-based scenarios. It was found that energy losses directly related to  
hydrogen production would be in the order of 50% of the generated energy, and that storage and transportation costs would  
70 account for nearly half of the cost of the fuel. In contrast, the other possible energy vector options (synthetic natural gas  
(SNG), methanol, or Fischer-Tropsch fuel (FT fuel) (Graves et al., 2011) and ammonia (Morgan, 2013) are much simpler to  
store, transport and distribute (particularly methanol and FT fuel, as they are liquid for standard conditions of temperature  
and pressure). Moreover, they can be incorporated into existing infrastructure with little to no modification. The drawback is  
that they each require the supply of an additional feedstock (carbon dioxide or nitrogen depending on the energy vector) and  
75 an additional conversion step in the energy conversion process. The additional conversion step decreases the overall energy  
efficiency and increases the size and complexity of the PtX plant. In a previous study (Babarit et al., 2019), we investigated  
whether these drawbacks could be compensated by the easier storage, transportation and distribution of the products, and  
found that methanol is the most promising solution; hence it is retained as the energy vector in this study.

It can be noted that Kim & Park were the first to suggest methanol production for energy ships (Kim and Park, 2010).  
80 However, their design is based on large kite sails flown at high altitude, a technology which does not exist as of today. In  
contrast, we propose to use Flettner rotors, a technology which is commercially available (Norsepower, 2019), which is  
characterized by high aerodynamic performance (lift coefficient over 12 have been measured in experiments (Charrier,  
1979), which is easy to control (the lift depends on only one control variable which is the rotor's rotational velocity) and  
which is inherently fail-safe (the aerodynamic loads are minimal when the rotors are stopped such as in the case of failure).



85

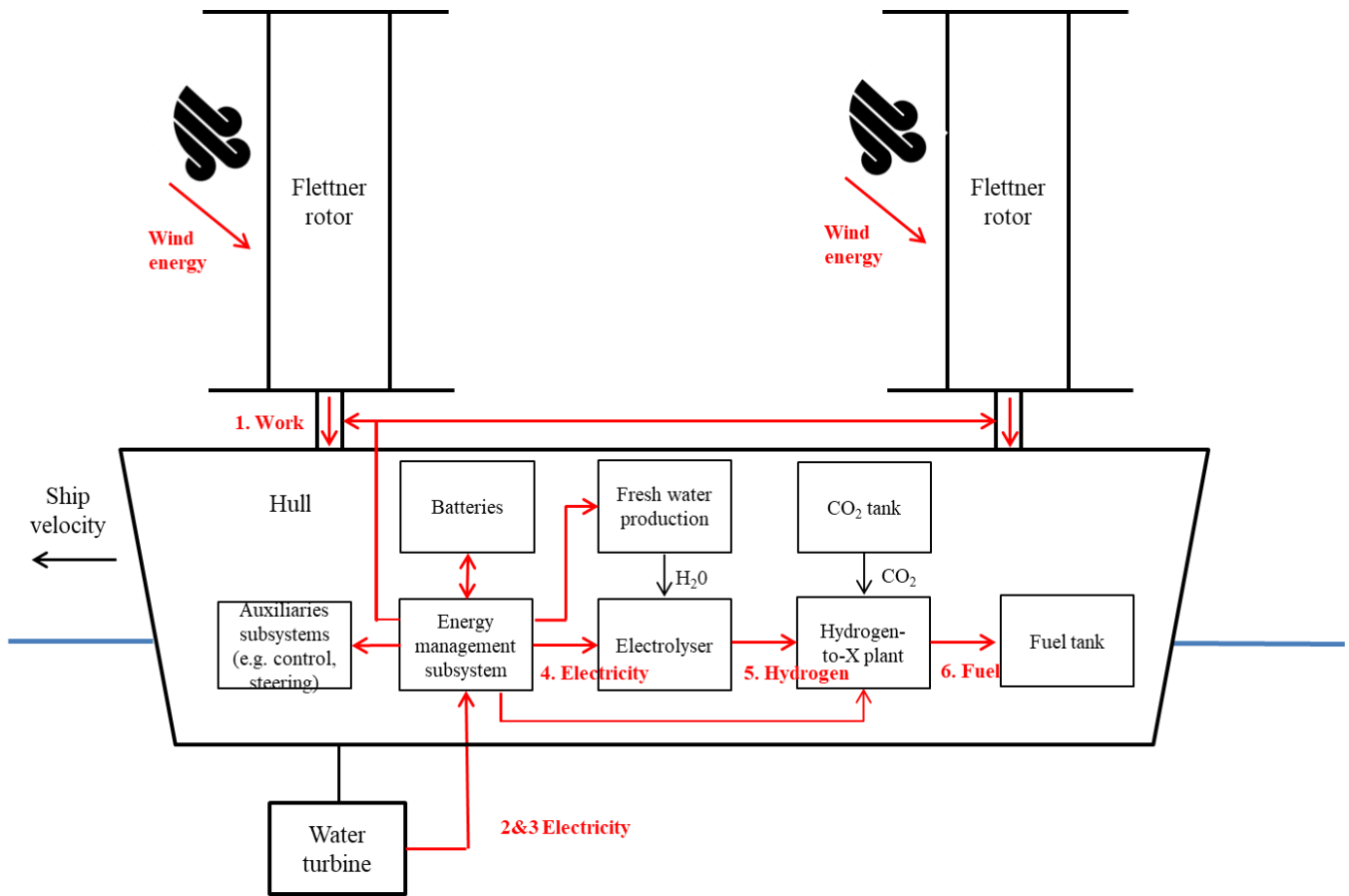
**Figure 2** The concept of sustainable methanol production from far-offshore wind energy by FARWIND energy systems.

A second difference with the works of Kim & Park is that we propose that the energy ships are deployed in fleets in order to produce large volumes of fuel; and that the produced methanol is collected by tankers which are also used to supply the energy ships with the necessary feedstock (carbon dioxide) for power-to-methanol conversion, see Fig. 2. We call this energy system “FARWIND”. Obviously, the CO<sub>2</sub> supply source must be sustainable for that system to produce sustainable methanol. Therefore, it must be captured directly or indirectly from the atmosphere. Nowadays, there are several possible options including direct air capture (Keith et al., 2018), CO<sub>2</sub> capture from flue gases from biomass or FARWIND-produced methanol combustion, and CO<sub>2</sub> from biogas upgrading (Li et al., 2017; Irlam, 2017).

The overall aim of the present study is to investigate the energy and economic performance of the proposed FARWIND energy system. The present paper deals with the energy ship design and its energy performance. The economic performance of the whole system is analyzed in a related paper (Babarit et al., submitted).

The remainder of this paper is organized as follows. In section 2, the energy conversion process from wind energy to methanol aboard an energy ship is described and mathematical models for each conversion stage are proposed. The models are quite similar to those proposed in (Kim and Park, 2010; Platzer et al., 2013; Pelz et al., 2016; Gilloteaux and Babarit, 2017; Ouchi and Henzie, 2017). However, fundamental results regarding the effect of the water turbine on the energy conversion efficiency are highlighted which were not in previous studies. In section 3, the specifications of the proposed energy ship are presented. Its energy performance and efficiency are discussed in section 4. Section 5 is the conclusion of the paper.

## 2 Models of the processes and energy flow in a methanol-producing energy ship



105

Figure 3 Description of the energy flows in a methanol-producing energy ship. Note that in this schematic, the wind propulsion subsystem are Flettner rotors. However, other sail concepts can be used.

### 2.1 General description of the energy flow in a methanol-producing energy ship

Fig. 3 shows a description of the wind energy to methanol conversion process in a methanol-producing energy ship. It includes seven elementary conversion stages:

- Conversion of wind energy into work by the a wind propulsion subsystem (Flettner rotors in the present study, see section 3.1).
- Conversion of the work into mechanical energy by the rotor of the water turbine.
- Conversion of the mechanical energy at the shaft of the water turbine into electricity.
- Management of the electricity aboard the energy ship. Some of the produced electricity will be used to power auxiliary subsystems that are required for the operation of the energy ship (e.g. the control and steering subsystem).
- Fresh water production for hydrogen synthesis

115

- Conversion of electricity into hydrogen by the electrolyzer.
- Conversion of hydrogen into methanol by the methanol synthesis plant.

120 The first three elementary conversion stages, allowing wind power to be converted into electrical power, are strongly coupled (see next section), and are collectively defined as the wind-to-electricity subsystem.

The last three elementary stages, corresponding to the conversion of electric power into methanol, are the power-to-methanol subsystem. This includes the electrolyzer, the methanol synthesis unit and a freshwater production unit, which is necessary to supply water to the electrolyzer.

125 The third key subsystem, corresponding to the fourth elementary conversion stage, is the energy management subsystem. Albeit not strictly speaking a conversion stage, this stage is pivotal to articulate the two other stages.

In the following, models are presented for these three subsystems.

## 2.2 Model for the wind-to-electricity subsystem

The first conversion stage is the conversion of wind energy into propulsive work by the the wind propulsion subsystem. The corresponding propulsive power,  $P_1$ , is equal to the product of the thrust force  $T$  (the component of the aerodynamic force along the axis of the ship) and the ship forward velocity  $U$ :

$$P_1 = TU \tag{1}$$

The drift velocity (the component of the ship velocity perpendicular to axis of the ship) is neglected.

The thrust force can be estimated from the wind speed according to:

$$T = \frac{1}{2} \rho_a A_s V^2 (C_L \sin \alpha - C_D \cos \alpha) \tag{2}$$

where  $\rho_a$  is the air density,  $A_s$  is the sail area (projected area),  $V$  is the apparent wind speed,  $\alpha$  is the apparent wind angle, and  $C_L$  and  $C_D$  are the lift and drag coefficients of the rig.

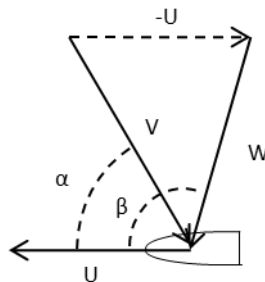


**Figure 4 Definitions of the true wind angle  $\beta$  and apparent wind angle  $\alpha$ .**

140 The apparent wind speed and the apparent wind angle derive from the true wind speed  $W$  and the true wind angle  $\beta$  (see Fig. 4) as follows:

$$\begin{cases} V^2 = U^2 + W^2 + 2UW \cos \beta \\ W \sin \beta = V \sin \alpha \end{cases} \quad (3)$$

The second conversion stage is the conversion of a part of the propulsive power into mechanical power  $P_T$  by the rotor of the water turbine. According to momentum theory (Manwell et al., 2009):

$$P_T = R_T(1 - a)U \quad (4)$$

where  $a \in [0,1]$  is the axial induction factor and  $R_T$  is the thrust force generated by the turbine. It can be written:

$$R_T = 2\rho_w A_T a(1 - a)U^2 \quad (5)$$

where  $\rho_w$  is the water density and  $A_T$  is the turbine disk area.

In order to understand the energy loss in this conversion stage, let us consider the forces acting on the ship. In addition to the force generated by the turbine, the other forces applying to the ship are the thrust force from the wind propulsion subsystem and the water resistance  $R_w$ . The water resistance corresponds to the effect of the water resisting the forward motion of the ship (hull resistance). According to (ITTC, 2014), the water resistance  $R_w$  can be written:

$$R_w = [(1 + k)C_f + C_R] \frac{1}{2} \rho_w A_v U^2 \quad (6)$$

where  $C_f$  is the frictional resistance coefficient,  $C_R$  is the residuary resistance coefficient,  $k$  is the form coefficient and  $A_v$  is the wetted area of the ship's hull. Since the form coefficient  $k$  is usually small, it is neglected in this study. The frictional resistance coefficient can be estimated using the ITTC-1957 formula:

$$C_f = \frac{0.075}{(\log_{10} Re - 2)^2} \quad (7)$$

where  $Re$  is the Reynolds number.

The residuary resistance coefficient can be calculated using dedicated software; in this study, REVA was used (Delhommeau and Maisonneuve, 1987).

In steady state, the thrust force is equal to the turbine force plus the water resistance:

$$T = R_T + R_w \quad (8)$$

Using equations (2), (3), (5) and (6) in equation (8), it can be shown that:

$$\frac{\rho_a}{\rho_w} \left( \sin \alpha - \frac{C_D}{C_L} \cos \alpha \right) V^2 = \left[ \left( \frac{C_f}{C_L} + \frac{C_R}{C_L} \right) \frac{A_v}{A_s} + 4 \frac{A_T}{A_s} \frac{1}{C_L} a(1 - a) \right] U^2 \quad (9)$$

165 This last equation gives a relation between the ship velocity  $U$  and power absorption by the water turbine (through the axial induction factor  $a$ ). In other words, the ship velocity depends on how much power is absorbed by the turbine.

Combining equations (4) and (5), the power absorbed by the water turbine can be written in the classical form:

$$P_T = 2\rho_w A_T a(1-a)^2 U^3 \quad (10)$$

170 The fundamental difference between energy ships and fixed wind or marine current turbines is that the velocity  $U$  depends on the axial induction factor. Thus, the optimal induction factor depends on the particulars of the energy ship design. Fig 5. shows an example of the ship velocity and absorbed power as function of the induction factor. The true wind speed is 10 m/s and the true wind angle is  $90^\circ$ . For this example, one can see in Fig. 5 that the optimal induction factor is approximately 0.04, which is much smaller than the optimal induction factor for fixed turbines of  $a = \frac{1}{3}$ , given by Betz theory. To our knowledge, Pelz et al. (Pelz et al., 2016) were the first to point out that this aspect is a key optimization parameter of the energy performance of energy ships. In contrast, this was not realized by Kim & Park (Kim and Park, 2010; Kim and Park, 2014), who assumed  $a = \frac{1}{3}$  in their studies. This is an important point, as it can lead to the underestimation of the absorbed power (as can be seen in Fig. 5 in which the absorbed power for  $a = \frac{1}{3}$  is more than two times less than that for the optimal induction factor).

180 Let us define the energy efficiency of the second energy conversion stage (conversion of propulsive power into mechanical power on the shaft of the water turbine) by:

$$\eta_2 = \frac{P_T}{P_1} \quad (11)$$

Recalling that  $P_1 = TU$  and using equations (4), (5) and (7) in (10), one can show:

$$\eta_2 = \frac{2\rho_w A_T a(1-a)^2}{[(1+k)C_f + C_R] \frac{1}{2} \rho_w A_v + 2\rho_w A_T a(1-a)} \quad (12)$$

which can be rewritten:

$$\eta_2 = 1 - \frac{[(1+k)C_f + C_R] \frac{1}{2} \rho_w A_v + 2\rho_w A_T a^2(1-a)}{[(1+k)C_f + C_R] \frac{1}{2} \rho_w A_v + 2\rho_w A_T a(1-a)} \quad (13)$$

185

Thus, using equations (4), (5) and (7), one can show:

$$\eta_2 = 1 - \frac{R_w}{T} - a \frac{R_T}{T} \quad (14)$$

This equation shows that the energy loss in the second conversion stage has two origins. The first is obviously the resistance of water to the forward motion of the ship. The second—less obvious—is proportional to the turbine force times the axial induction factor. This can be explained by the fact that the water turbine does not only convert wind energy into mechanical energy, but also transfers some of that energy to the water that it passes through. Indeed, in contrast to a wind turbine or a marine current turbine, the water turbine rotates in water that is initially at rest. Once the ship has passed, some of that water has been set in motion. The second energy loss in equation (14) corresponds to the kinetic energy transferred to that body of water.

In practice, it may be desirable to maximize the energy efficiency  $\eta_2$ . Using equation (13) and elementary algebra, one can show that  $\eta_2$  increases monotonically with increasing water turbine area  $A_T$ , and that:

$$\lim_{A_T \rightarrow \infty} \eta_2 = 1 - a \quad (15)$$

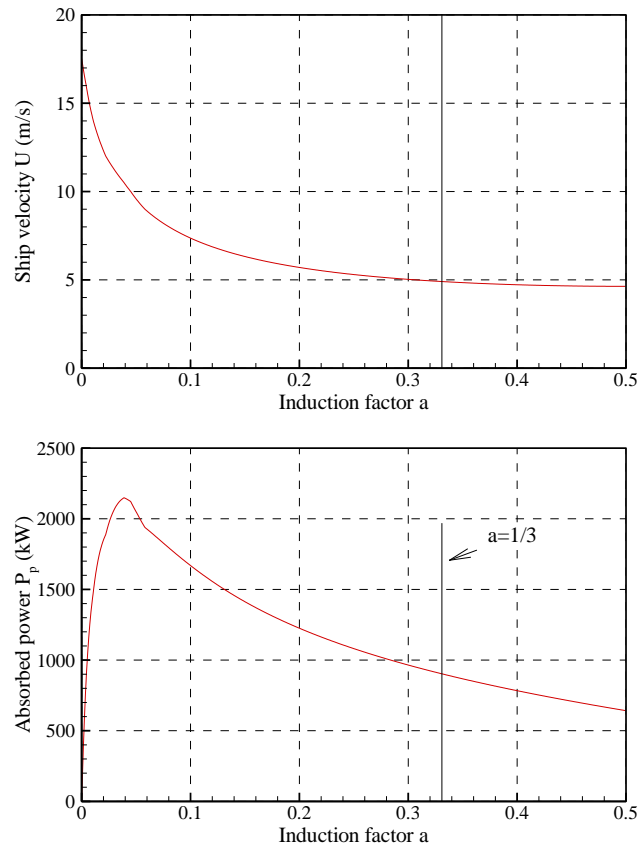
Thus, the efficiency of conversion of wind energy into mechanical energy by energy ships is limited to  $\eta_2 = 1 - a$ . Maximization of the energy efficiency of this conversion stage requires the water turbine area to be large and the axial induction factor to be small. In particular, one can see that setting  $a = \frac{1}{3}$  would limit the efficiency to less than 67%.

Fig. 6 shows an example of the absorbed power and efficiency  $\eta_2$  as function of the water turbine diameter. One can see that, as expected, the efficiency increases with increasing turbine diameter. However, the rate of increase in efficiency diminishes with increasing turbine diameter, which is worth noting as turbine cost will also increase with increasing diameter. Therefore, despite theory indicates that as large as possible water turbine should be used, turbines of practical dimensions may be used with little efficiency loss.

The third conversion stage is the conversion of the mechanical energy extracted by the rotor of the water turbine into electricity by a generator. The energy efficiency of this conversion stage is denoted  $\eta_3$ . Energy losses in this stage include friction and drag on the blades of the turbine, mechanical losses, generator losses, etc.. This efficiency is approximately 80% for wind turbines (Burton et al., 2001). It is assumed that a similar efficiency can be achieved for the water turbines of energy ships.

The electricity generated by the water turbine  $P_e$  as function of the true wind speed and wind direction can be estimated using:

$$P_e = 2\eta_3\rho_w A_T a(1 - a)^2 U^3$$



**Figure 5 Ship velocity (top) and absorbed power (bottom) as function of the induction factor. The true wind speed is 10 m/s and the true wind angle is 90°. The wind propulsion subsystems are Flettner rotors. The spin ratio is 3. Constraints on maximum rotational velocity, maximal thrust and cut-out speed are not taken into account in this example.**

215

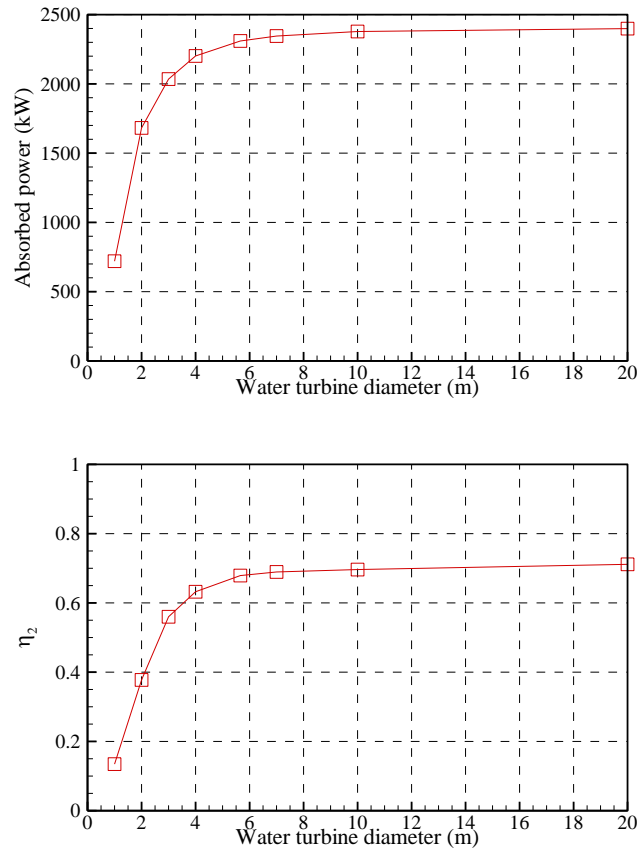


**Figure 6 Absorbed power (top) and propulsion power to water turbine mechanical power (bottom) as function of the water turbine diamer. The true wind speed is 10 m/s and the true wind angle is 90°. The wind propulsion subsystems are Flettner rotors. The spin ratio is 3. Practical constraints on maximum rotational velocity, maximal thrust and cut-out speed are not taken into account in this example.**

220

### 2.3 Model for the energy management subsystem

The energy management subsystem is an important subsystem in an energy ship. The main function of this system is to supply energy to all auxiliary subsystems that are required for their operation, for example the control and steering subsystem or navigation lights. It also supplies energy for the control and spinning of the Flettner rotors.

225

The energy management subsystem is expected to include batteries, which will be used to maintain maneuvering and communication capabilities in the absence of wind. Thus, during power production, it is expected that a small part of that power will be used for charging the batteries.

The efficiency  $\eta_4$  of this stage is defined as the ratio of the remaining electricity available to feed the power-to-methanol plant to the electricity produced by the generator:

230

$$\eta_4 = 1 - \frac{P_{aux}}{P_e} \quad (16)$$

where  $P_{aux}$  is the power consumed by auxiliary subsystems.

## 2.4 Model for the power-to-methanol subsystem

The power-to-methanol subsystem includes two main stages: the conversion of electricity into hydrogen by an electrolyzer,  
235 and the conversion of hydrogen and carbon dioxide into methanol.

### 2.4.1 Electrolyzer

Using electricity, water can be separated into hydrogen and oxygen:



Electrolysis technologies include alkaline electrolysis (AEL), polymer electrolyte membrane (PEM) electrolysis and solid  
240 oxide electrolysis (SOEC). Of these, AEL is the most mature technology (Gotz et al., 2016). AEL electrolyzers can last for 30 to 40 years. Their design capacity is in the MW range. They can be operated between 20 and 100% of their design capacity, and capacity can be varied from 20 to 100% in approximately 10 minutes (Agersted, 2014). Their use in the offshore environment was studied in the H2OCEAN European project (Agersted, 2014), which concluded that it is feasible. Thus, the AEL technology has been retained for the FARWINDERS.

245 According to (Gotz et al., 2016), the power consumption of AEL electrolyzers is in the order of 55 kWh per kg of produced hydrogen. The corresponding energy efficiency  $\eta_5$  is 60%, based on the lower heating value of hydrogen (approx. 33 kWh/kg). The water consumption is 9 kg of fresh water per kg of hydrogen.

It can be noted that performance of water electrolysis technology is expected to improve in the coming decade. According to  
250 (Schmidt et al., 2017), the energy efficiency of AEL technology may increase up to 67%, and PEM technology may reach even greater efficiencies while achieving similar lifetime to AEL technology. Moreover, despite PEM would still be more expensive than AEL, it has been shown that the advantage in efficiency may lead to better overall financial performance (McDonagh et al., 2018). Therefore, the efficiency data used in this paper can be considered as conservative and PEM electrolyzers may eventually be a better option than AEL for the FARWINDERS.

### 2.4.2 Hydrogen-to-methanol plant

255 In the hydrogen-to-methanol plant, hydrogen is combined with  $CO_2$  in order to produce methanol (and water as a by-product).

In practice, there are two processes available for methanol synthesis using CO<sub>2</sub> and hydrogen as the reactants (Anicic et al., 2014; Connolly et al., 2014): two-step methanol synthesis (CAMERE process) and direct methanol synthesis (CO<sub>2</sub> hydrogenation). The first step in the two-step process is the production of syngas (a mixture of carbon monoxide, carbon dioxide, and hydrogen) through the reverse water-gas shift reaction and water separation. The syngas is subsequently converted into methanol. Note that, at present, methanol is produced industrially at large scale from syngas (Machado et al., 2014) obtained from methane through steam reforming. In contrast, in the direct methanol synthesis process, the methanol is obtained directly from CO<sub>2</sub> and H<sub>2</sub> via the reaction:



The direct process is currently used in the George Olah power-to-methanol plant, which can produce 4,000 tonne per annum (Marlin et al., 2018). The process was modeled in (Machado et al., 2014). The temperature is 245°C and pressure 80 bars. Results show that the power consumption is 0.93 kWh per kg of methanol, and CO<sub>2</sub> consumption is approximately 1.38 kg per kg of methanol. According to (Marlin et al., 2018) and (Anicic et al., 2014), the direct methanol synthesis process is more energy-efficient than the two-step process. Moreover, according to (Anicic et al., 2014), the production cost is comparable in the two processes. Therefore, the direct process is selected for the power-to-methanol plant of the FARWINDERS.

The efficiency  $\eta_6$  of this last conversion stage is the ratio of the lower heating value of the produced methanol (5.54 kWh/kg<sub>MeOH</sub>) to the sum of the lower heating value of the input hydrogen (6.19 kWh/kg<sub>MeOH</sub>) and the power consumption (0.93 kWh/kg<sub>MeOH</sub>). Thus, the efficiency  $\eta_6$  is 78%.

### 275 **2.4.3 Fresh water production**

The electrolyzer requires a fresh water supply of 1.69 kg/kg<sub>MeOH</sub>. This can be provided by desalinating seawater, either through reverse osmosis or through distillation. According to (Fasihi et al., 2016), the power consumption is in the order of 3 kWh/m<sup>3</sup> using reverse osmosis, corresponding to a negligible 3.4 Wh/kg<sub>MeOH</sub>. Moreover, methanol synthesis also results in water production (see Equation (18)). Thus, a third of the freshwater needs could be met through water recycling. Although freshwater production does not contribute significantly to parasitic energy demande, freshwater recycling may improve system maintenance and lifetime.

### 2.4.4 Assembled model of the power-to-methanol plant

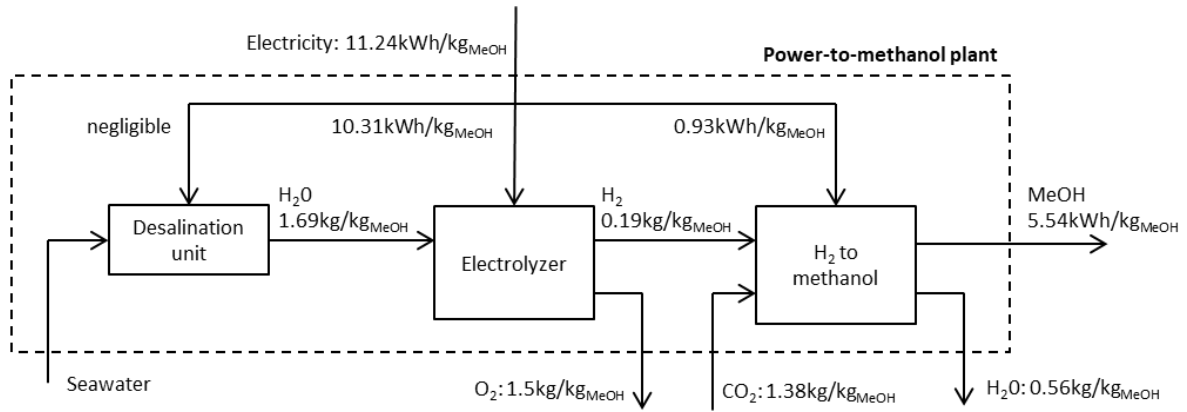


**Figure 7 Assembled model for the power-to-methanol plant**

285 Fig. 7 shows the assembled model for the power-to-methanol plant and the process flows. One can see that it takes 1.38 kg of  $\text{CO}_2$  and 11.24 kWh of electricity to produce 1 kg of methanol. The energy efficiency  $\eta_7$  is thus 49% (not taking into account the energy required to produce the  $\text{CO}_2$ ).

### 3 Development and specifications of the proposed energy ship design

290 The model presented in section 2 allows the power production of a FARWINDER to be calculated as function of the wind conditions (true wind angle  $\beta$ , true wind speed  $W$ ). As explained in that section, the induction factor  $a$  can be optimized in order to maximize energy production. Moreover, energy production depends on the thrust force of the chosen wind propulsion subsystem (Flettner rotors, see section 3.1), which itself depends on their rotational velocity. Therefore, a numerical program was developed to determine the optimal induction factor and rotational velocity as function of the FARWINDER design and the wind conditions. A brute-force search was used for the optimization. The constraints on the maximum rotational velocity of the Flettner rotors, maximum thrust on the rotors as well as maximum power of the generator of the water turbine are taken into account through penalization in the optimization loop.

295 Using this model, we have developed, investigated and optimized a number of energy ship designs over the last two years. The details of this process are not reported here for sake of conciseness.

300 Instead, we focus on the most promising design that has been achieved. It consists of an 80 m long catamaran with four 30 m tall Flettner rotors, and two water turbines with rated power 900 kW each, see Fig. 8. The complete specifications of this design are given in Tab. 1. The reasons for the design choices are explained in the following sections.

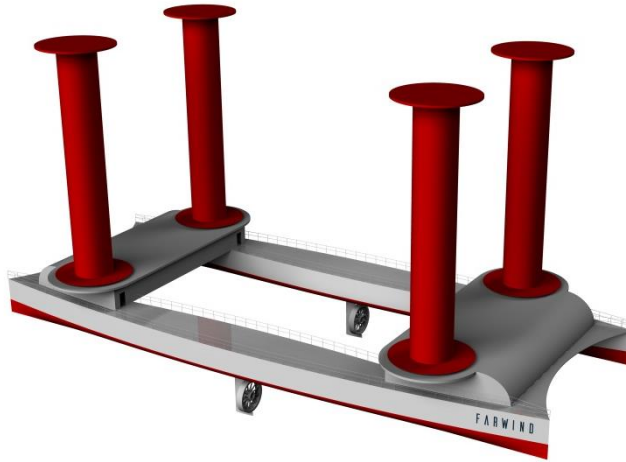


**Figure 8 Artist's view of the proposed energy ship design.**

	Unit	Value
<b>Hull</b>		
Length	m	80
Breadth	m	31.7
Draught	m	1.6
Displacement	t	660
Structural mass	t	258
<b>Wind propulsion</b>		
Type	-	Flettner rotors
Number	-	4
Rotor height	m	30
Rotor diameter	m	5
Rotor mass	t	59
Rotor rated power	kW	110
<b>Water turbine</b>		
Number	-	2
Rotor diameter	m	4
Rotor-to-electricity efficiency ( $\eta_3$ )	-	80%
Turbine mass	t	7.4
Rated power	kW	900
<b>Auxiliaries subsystems</b>		
Power consumption	kW	50
Auxiliaries subsystems mass	t	32
<b>Power-to-methanol plant</b>		

Electrolyzer rated power	kW	1,420
Electrolyzer mass	t	35
Desalination unit rated power	kW	Negligible
Desalination unit mass	t	Negligible
H <sub>2</sub> tMeOH plant capacity	kg/h	138
H <sub>2</sub> tMeOH plant mass	t	24
Storage tanks		
CO <sub>2</sub> storage capacity	t	32
Storage tank mass (empty)	t	21
Methanol storage capacity	t	23
Storage tank mass	t	5

**Table 1 Specifications of the proposed energy ship design**

305

### 3.1 Wind propulsion subsystem

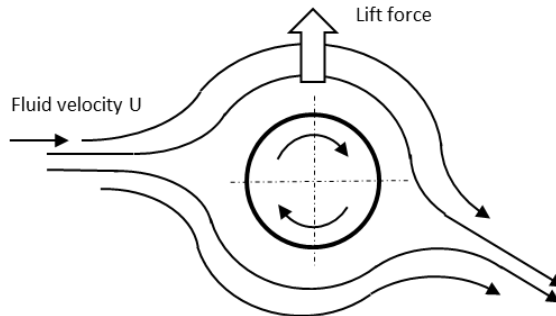
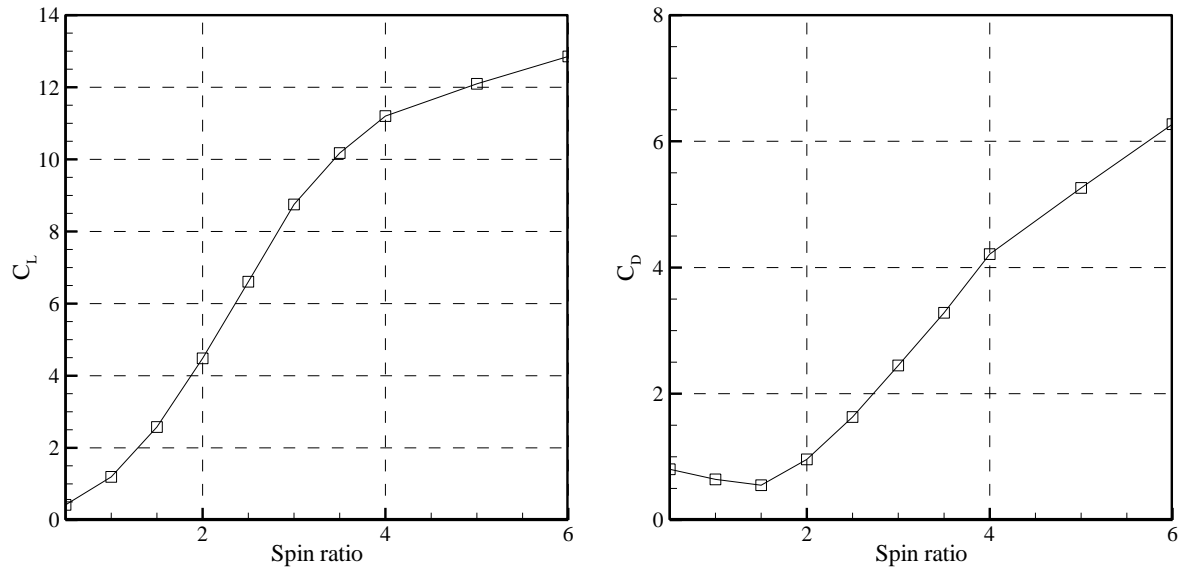


**Figure 9 On the left, the “E-Ship 1” in 2015. It is fitted with four 27 m tall Flettner rotors. Picture by Alan Jamieson. On the right, diagram showing the Magnus effect by which lift is produced by a rotating cylinder.**

310 Flettner rotors were selected for the rigging. A Flettner rotor is a rotating vertical cylinder whose axis is perpendicular to the wind. Due to the Magnus effect, the action of the wind on the cylinder generates a lift force perpendicular to both the wind direction and the axis of the cylinder. Fig. 9 shows a picture of an existing wind-assisted propulsion cargo ship, the “E-ship 1”, which is fitted with four 27 m tall rotors.



315 **Figure 10** Experimental results of Charrier (Charrier, 1979) for the aerodynamic coefficients of a Flettner rotor. Left figure is the lift coefficient. The right figure shows the drag coefficient. In the experiments, the rotor was fitted with end discs at both ends. The diameter of the discs was twice the diameter of the rotor. The aspect ratio of the rotor was 5 and the Reynolds number was 13,200.

320 Fig. 10 shows the experimental results of Charrier (Charrier, 1979) for the aerodynamic coefficients of a Flettner rotor as function of the spin ratio  $\alpha$  (ratio of rotation speed to wind speed). In the experiments, the rotor was fitted with end discs at both ends. The diameter of the discs was twice the diameter of the rotor. The aspect ratio of the rotor was 5 and the Reynolds number was 13,200.

325 Flettner rotors are commercially available from the company Norsepower (Norsepower, 2019). Their tallest rotor is 30 m, having diameter 5 m and weight 59 t. The maximum thrust is 270 kN and the maximum rotational velocity is 180 rpm. Note that rotors need to be powered to be able to spin, which is a drawback of Flettner rotors. The rated power of the electric motor driving the rotor is 110 kW for the 30 m tall rotor. However, in practice, it has been observed that the average rotor's power consumption is significantly less than the rated power (International Wind Ship Association, 2019). In this study, an average power consumption of 40 kW has been used following advice from Norsepower (Kuuskoski, 2019).

### 3.2 Hull



**Figure 11** The HMAS “Jervis Bay” in 2000.

330

Equation (1) shows that energy ships should sail fast to maximize the absorbed power from the wind. Moreover, equation (14) shows that hull resistance is detrimental to the energy efficiency of energy ships. For these reasons, an 80 m-long, 31.7 m-wide catamaran hull shape was selected, inspired by the 86 m-long 26 m-wide HMAS Jervis Bay wave-piercing catamaran (Fig. 11). It can be noted that the displacement of the HMAS Jervis Bay is 1,250 t.

335

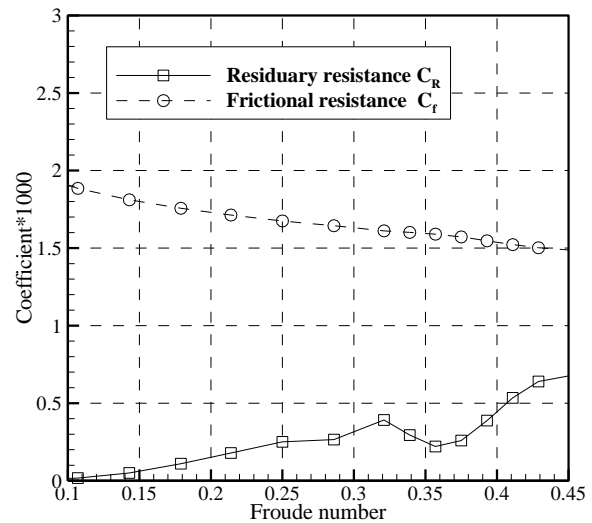
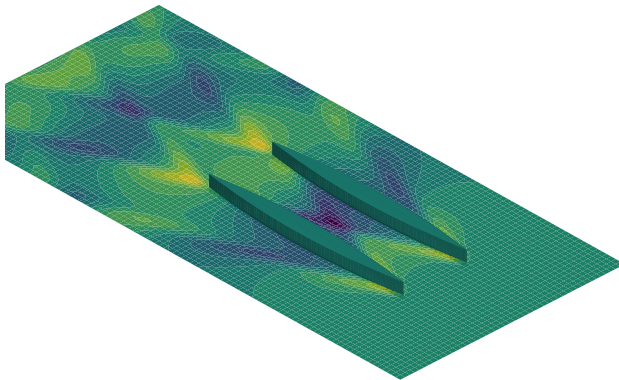


**Figure 12** Picture of the hull shape considered in this study and related hydrodynamic coefficients

Fig. 12 shows the shape and resistance coefficients of the proposed energy ship hull, whose displacement is 660 t. The shape of the floaters is based on the Wigley hull, which is defined by:

340

$$y(x, z) = \frac{B}{2} \left(1 - \left(\frac{z}{T}\right)^2\right) \left(1 - \frac{4x^2}{L^2}\right) \quad (19)$$

where B is the breadth, T is the depth and L is the length. In this study, the parameters are set to B = 6.67 m, T = 1.88 m and L = 80.0 m.

The frictional resistance coefficient was calculated according to equation (7), and the residuary (wave) resistance coefficient was obtained using the REVA software (Delhommeau and Maisonneuve, 1987). As shown in Fig. 12, the frictional resistance coefficient is an order of magnitude greater than the residuary resistance coefficient. This was expected as the hull shape is very thin.

The structural mass is set to 258 t. Note that it is not based on a structural analysis; rather, it was estimated by taking the difference between the displacement (660 t) and the total mass of all equipment installed onboard plus the mass of the CO<sub>2</sub> contained in the CO<sub>2</sub> storage tank when it is full. Therefore, an important question is whether this structural mass is sufficient to ensure that the ship can withstand harsh ocean conditions, especially in the windy areas where energy ships are expected to be deployed. To address this question, we note that the ratio of structural mass to total displacement for (steel) merchant ships is in the range 10 to 40% (Papanikolaou, 2014), the lower values corresponding to large cargo ships and the higher values ferries and passengers ships. For the energy ship design considered in this study, the ratio is 39%, thus in the higher end of the range. Moreover, the energy ships' structure may be made of GFRP or aluminium, which requires less structural weight than steel for the same structural strength. Therefore, we expect that the current provision for structural mass will be sufficient. This needs to be validated in future work.

### 3.3 Water turbine

The requirements for the energy ships' water turbines are a rated power of 900 kW each, a rated flow velocity of 10.5 m/s (see section 4.1), and a large swept area  $A_T$  in order to maximize efficiency (according to equation (13)). Unfortunately, to our knowledge, there is no water turbine commercially available whose specifications match these requirements. Indeed, the required rated power (MW-scale) is much greater than commercial hydro-generators for sailing boats (kW-scale). The rated power of tidal turbines is similar to the energy ship's requirements, however their flow velocity is significantly lower (~3 m/s (Atlantis Resources, 2019)). Therefore, appropriate dimensions and characteristics for the turbines can only be estimated.

The AR1500 tidal turbine developed by the company Simec Atlantis (Atlantis Resources, 2019) has rated power 1.5 MW, flow velocity 3 m/s, diameter 18 m (corresponding to 254 m<sup>2</sup> swept area) and mass 150 t. Since the rated flow velocity of energy ships is expected to be in the order of 10 m/s, much smaller turbines can be used to achieve MW-scale power generation; however, turbines with large diameter are expected to be beneficial to the energy ship's efficiency according to equation (13). Thus, a turbine diameter of 4 m (25 m<sup>2</sup> total swept area for the two turbines) was selected. According to equation (10), an axial induction factor of  $a=0.04$  is required to achieve a power generation of approximately 1.8 MW for a flow velocity of 10.5 m/s. It can be noted that this is an order of magnitude less than for wind turbines.

According to (Sanchez de Lara Garcia, 2013), the nacelle mass of a wind turbine is approximately proportional to the square of the turbine diameter. Recalling that the AR1500 tidal turbine nacelle mass is 150 t and its diameter is 18m, the mass of a 4 m diameter water turbine is estimated to be in the order of 7.4 t.

### 375 **3.4 Power-to-methanol plant**

Containerized AEL electrolyzers are commercially available from the company Nel Hydrogen (C-series). The Nel C-150 eletrolyzer has a capacity of 150 Nm<sup>3</sup>H<sub>2</sub>/h, corresponding to a rated power of approximately 750kW for 60% efficiency. According to (Agersted, 2014), the weight of a 2,400 kW electrolyzer is 60 t. Thus, we estimate that the 1,420 kW-rated power electrolyzer required for the proposed energy ship design will have a weight of 35 t.

380 For the H<sub>2</sub>-to-methanol plant, the company INERATEC develops compact containerized chemical plants that could be used for energy ships. The weight is in the order of 28 t for a 1 MW rated power capacity (Schulz, 2019). Thus, we estimate that the plant required for the FARWINDER, having power capacity 850 kW-rated, would have weight 24 t.

### **3.5 Storage tanks**

385 Since energy ships are mobile, their route schedules can be dynamically optimized based on weather forecasts in order to maximize energy production. This was performed by Abd-Jamil et al. (Abd-Jamil et al., 2019) for a 1 MW energy ship deployed in the North Atlantic Ocean, assuming the arrival point to be the same as the starting point, whose coordinates are: N 54.51660; W 27.551844 (mid-distance between Ireland and Newfoundland, Canada). Over the three years 2015, 2016 and 2017, it was found that an average capacity factor of over 80% can be achieved. Moreover, they found that the average duration of the routes is six days.

390 The performance of the energy ship considered in this study is similar to that of Abd-Jamil et al. (see section 4.1). Therefore, we consider that the storage tanks should be designed to be able to accommodate seven days at full capacity, corresponding to a capacity of 32 t for the carbon dioxide tank and 23 t for the methanol tank.

395 Carbon dioxide is usually liquefied for transportation and storage (-20°C temperature, 20 bars pressure). According to (Chart, 2019), the empty weight of a 26.8 t capacity vessel for liquid CO<sub>2</sub> storage is 18 t. For methanol, the weight of a tank of 15,000 gallons capacity (45 t) is 9 t. Thus, we estimate tank weights of 21 t for the liquid CO<sub>2</sub> storage tank and 5 t for the methanol storage tank.

### **3.6 Auxiliary equipment**

Auxiliary equipment includes mainly that required for navigation, control and communication subsystems (although this is not an exhaustive list). To account for their mass, the total mass budget excluding the hull mass is increased by 10% (34 t).

## 4.1 Power production charts

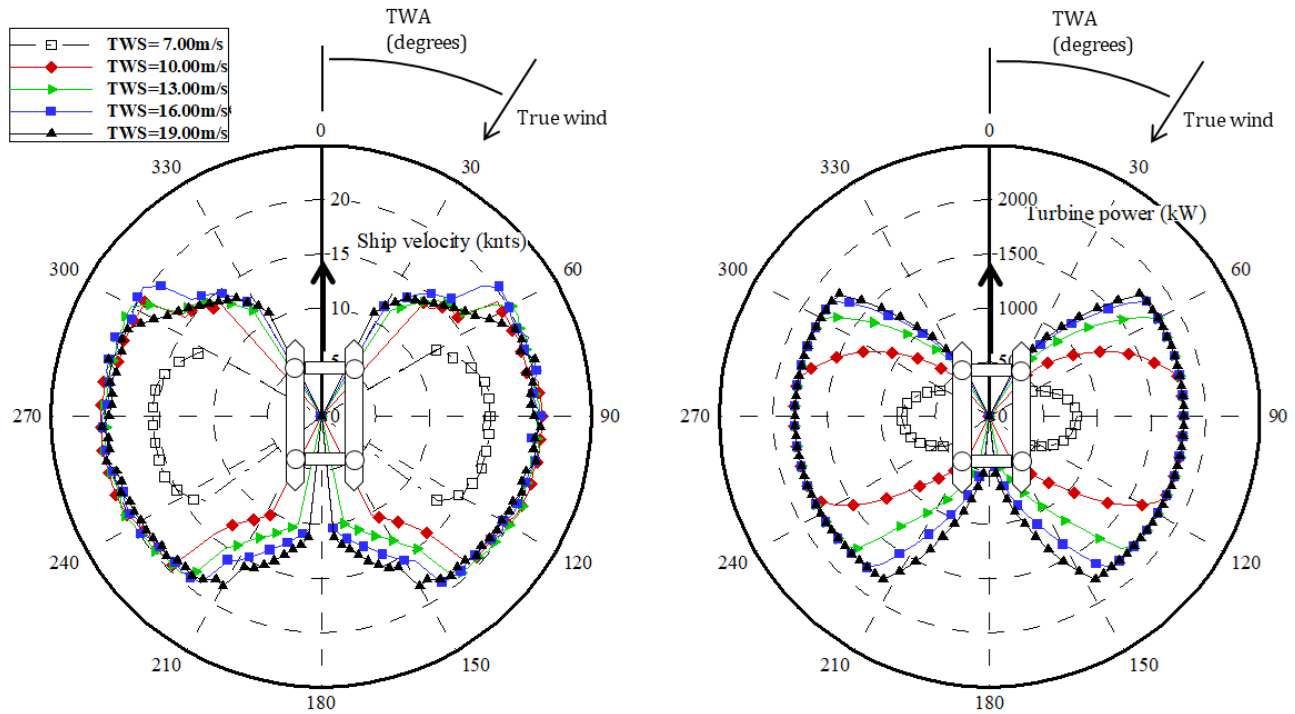


**Figure 13** Velocity (left) and generated power (right) polar plots of the proposed energy ship design for true wind speeds of 7, 10, 13, 16 and 19 m/s. TWA stands for true wind angle.

405 The velocity and the generated power of the proposed FARWINDER are shown in Fig. 13. Five values for true wind speed were considered: 7, 10, 13, 16 and 19 m/s (corresponding to wind forces on the Beaufort scale of 4, 5, 6, 7 and 8, respectively). Note that for each datapoint, the water turbine's induction factor and the rotors' spin ratio were optimized in order to maximize power production while satisfying the constraints (maximum rotation velocity and thrust force for the rotors, maximum power generation for the water turbine).

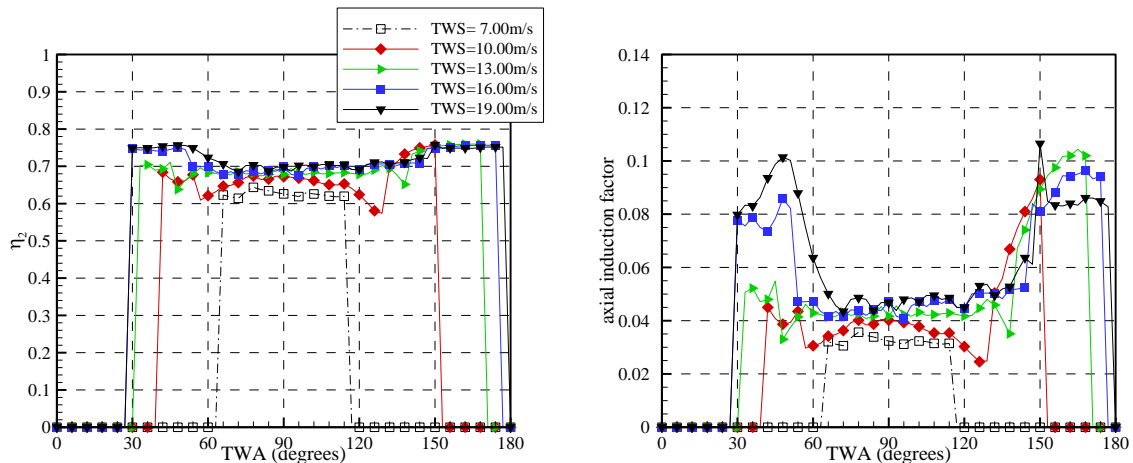
410 The right plot shows that in terms of optimizing power production, the most favorable wind direction is beam wind, particularly for lower wind speeds. Rated power production is achieved for wind speed slightly greater than 10 m/s. It can be observed that the range of wind directions for which rated power production is achieved widens with increasing wind speed. Overall, the FARWINDER is able to operate at full capacity in a great range of wind conditions.

The left plot shows that ship velocity is in the order of 20 knots (10.5 m/s) when the FARWINDER operates at full capacity.

415 This velocity is less than half that of the HMAS Jervis Bay wave-piercing catamaran, and corresponds to a Froude number of

0.37, which is well-aligned with typical Froude numbers for ships. It can be observed that velocity decreases with decreasing power.

## 4.2 Energy efficiency



420 **Figure 14 Efficiency of the conversion of wind energy into mechanical energy by the proposed energy ship design (left) and optimal induction factor (right) as function of the wind conditions. TWS stands for true wind speed.**

Fig. 14 shows the energy efficiency  $\eta_2$  of the wind-to-mechanical energy conversion stage (equation (14)) and the optimal induction factor as functions of wind direction for the five wind speeds. It can be seen that depending on the wind conditions, efficiency ranges from 60 to 75% and the optimal induction factor is in the range 0.02 to 0.11. In typical beam  
425 wind conditions, efficiency is in the order of 65-70%, and the optimal induction factor is 0.03 to 0.05, which is an order of magnitude smaller than for wind turbines. Taking into account the efficiency of converting mechanical energy into electricity,  $\eta_3=80\%$ , the overall efficiency of the wind-to-electricity conversion stage is typically 55%.

The power production available to the power-to-methanol plant is the power generated by the water turbine minus the power consumed by the auxiliaries and the Flettner rotors. In this study, it has been assumed that the power consumption of the  
430 Flettner rotors is 40 kW in all wind conditions. This leads to an efficiency of  $\eta_4=88\%$  for this energy management stage (equation (16)). Since the efficiency of the power-to-methanol plant is in the order of 49%, the overall wind-to-methanol efficiency is 24%.

## 4.3 Annual methanol production and CO<sub>2</sub> supply

In comparison to the power production polar plots of the FARWINDER considered in (Abd-Jamil et al., 2019), the energy  
435 ship proposed in this study is able to produce more power and in a greater range of wind conditions. Therefore, its capacity factor can be expected to exceed the value of 80% reported in (Abd-Jamil et al., 2019). However, that estimation did not take into account downtime due to planned and unplanned maintenance (availability). Therefore, the estimation of annual energy

production in the present study is based on a capacity factor of 75%, resulting in estimated methanol production of approximately 905 t per annum per energy ship (approximately 5 GWh per annum of chemical energy).

440 As the production of 1 kg of methanol requires 1.38 kg of CO<sub>2</sub>, the annual CO<sub>2</sub> supply must be 1,250 t per annum per energy ship.

## 5 Conclusions

In this paper, we presented a design of an energy ship which could be used to convert the far-offshore wind energy resource into sustainable methanol, and we investigated its energy performance. Its energy conversion efficiency (wind energy to  
445 methanol) is estimated to be 24%. The annual methanol production is estimated to be approximately 900 t per annum (5 GWh of chemical energy).

These energy ships could be deployed in fleets in order to enable large scale production of methanol. Methanol being a liquid fuel with rather high energy density, it could represent a sustainable viable substitute to fossil fuels for many uses (including transportation), provided that the CO<sub>2</sub> source is itself sustainable. However, there are several challenges to address  
450 first. A first challenge is the cost of energy. It is discussed in the related paper (Babarit et al., submitted). Other challenges include the development and validation of the key subsystems (water turbine, autonomous power-to-methanol plant, control systems for autonomous navigation) and addressing the possible non-technical barriers to far-offshore wind energy (legal status of autonomous far-offshore wind energy converters, environmental impacts).

## 6 Acknowledgements

455 This research was partially supported by the French National Energy and Environmental Agency (ADEME) and Région Pays de la Loire.

## 7 Data and code availability

The data generated during the current study are available from the corresponding author on request. Licences of the numerical program which was used to develop the proposed energy ship and assess its energy performance may be  
460 purchased from Ecole Centrale de Nantes.

## References

- Abd-Jamil, R., Chaigneau, A., Gilloteaux, J-C., Lelong, P., Babarit, A. : Comparison of the capacity factor of stationary wind turbines and weather-routed energy ships in the far-offshore. In *Journal of Physics: Conference series*, 1356, 2019
- Offshore wind programme board, *Transmission costs for offshore wind - final report*, April 2016
- 465 Agersted, K.: H2OCEAN D5.1 Report on expected marinised hydrogen generator performance. 157 pp., 2014
- Anicic, B., Trop, P., Goricanec, D.: Comparison between two methods of methanol production. *Energy*, 77, 279-289, 2014

- Atlantis resources . AR1500 Tidal turbine. Brochure, Atlantis resources. Available at: <https://www.atlantisresourcesltd.com/wp/wp-content/uploads/2016/08/AR1500-Brochure-Final-1.pdf> (Last accessed February 11, 2019)
- 470 Babarit, A., Gilloteaux, J-C. : Preliminary design of a wind driven vessel dedicated to hydrogen production. In Proc. of the ASME 36th International Conference on Ocean, Offshore and Arctic Engineering (OMAE2017), Trondheim, Norway, 2017
- Babarit, A., Gilloteaux, J-C., Clodic, G., Duchet, M., Simoneau, A., Platzer, M.F. : Techno-economic feasibility of fleets of far offshore hydrogen-producing wind energy converters. *International Journal of Hydrogen Energy*, 43(15), 7266-7289, 2018
- 475 Babarit, A., Gilloteaux, J-C., Body, E., Hetet, J-F.: Energy and economic performance of the FARWIND energy system for sustainable fuel production from the far-offshore wind energy resource. In Proc. Of the 14th International conference on ecological vehicles and renewable energies (EVER 2019), Monaco, 2019
- Babarit, A., Gilloteaux, J-C.: Sustainable methanol production from the far-offshore wind energy resource by fleets of energy ships. Part II. Cost of energy, Submitted
- 480 BP: BP Statistical review of world energy, 67<sup>th</sup> edition, June 2018
- Burton, T., Sharpe, D., Jenkins, N., Bossanyi, E.: *Wind energy handbook*. John Wiley & Sons, 2001
- Charrier, B. : Etude théorique et expérimental de l'effet « Magnus » destiné à la propulsion des navires. PhD thesis, Université de paris VI, 1979
- Chart, Technical manual: carbon dioxide storage tank. Manual #11650869 Rev
- 485 Chen, H., Ngoc-Cong, T., Yang, W., Tan, C., Li, Y., Ding, Y. : Progress in electrical energy storage system: a critical review. *Progress in Natural Science*, 19(3), 291-312, 2009
- Connolly, D., Mathiesen, B.V., Ridjan, I.: A comparison between renewable transport fuels that can supplement or replace biofuels in a 100% renewable energy system. *Energy*, 73, 110-125, 2014
- Delhommeau, G., Maisonneuve, J.J. : Extensions du code de calcul de résistante de vagues REVA: prise en compte des effets de fond et de portance. *Compte rendu des 1ères journées de l'hydrodynamique*, Nantes, 1987
- 490 Dupont, E., Koppelaar, R., Jeanmart, H. : Global available wind energy with physical and energy return on investment constraints. *Applied energy*, 209, 322-338, 2018
- Fasihi, M., Bogdanov, D., Breyer, C.: Techno-economic assessment of power-to-liquids (PtL) fuels production and global trading based on hybrid PV-wind power plants, *Energy procedia*, 99, 243-268, 2016
- 495 Gilloteaux, J-C., Babarit, A.: Preliminary design of a wind driven vessel dedicated to hydrogen production. In Proc. Of the ASME 2017 36th International conference on ocean, offshore and arctic engineering (OMAE), Trondheim, Norway, 2017
- Gizara, A.R.: Turbine-integrated hydrofoil. U.S. Patent 2007/0046028A1, 2007
- Gotz, M., Lefebvre, J., Mors, F., McDaniel Koch, A., Garf, F., Bajohr, S., Reimert, R., Kolb, T.: Renewable power-to-gas: a technological and economic review, *Renewable Energy*, 85, 1371-1390, 2016

- 500 Graves, C., Ebbesen, S.D., Mogensen, M., Lackner, K.S.: Sustainable hydrocarbon fuels by recycling CO<sub>2</sub> and H<sub>2</sub>O with renewable or nuclear energy. *Renewable and sustainable energy reviews*, 15, 1-23, 2011
- International WindShip Association – Quaterly newsletter february 2019
- Ioannou, A., Brennan, F.: A techno-economic comparison between a grid-connected and non-grid connected offshore floating wind farm, In Proc. Of the IEEE 2019 Offshore energy and storage summit (OSES), Brest, France, 2019
- 505 Keith, D.W., Holmes G., St Angelo, D., Heidel, K.: A process for capturing CO<sub>2</sub> from the atmosphere, *Joule*, 2, 1573-1594, 2018, 2018
- Kim, J., Park, C. : Wind power generation with a parawing on ships, a proposal, *Energy*, 35, 1425-1432, 2010
- Kim, J.C., Park, C.: Economy of hydrogen production by parafoil-pulled ships, *Journal of Energy Power Sources* Vol. 1(1), 9-16, 2014
- 510 Kuuskoksi, J.: Private communication, 2019
- Li, H., Tan, Y., Ditaranto, M., Yan, J., Yu, Z.: Capturing CO<sub>2</sub> from biogas plants, *Energy procedia*, 114, 6030-6035, 2017
- Irlam, L., Global costs of carbon capture and storage – 2017 update. Global CCS institute, June 2017
- ITTC: General guidelines for uncertainty analysis in resistance tests. ITTC – Recommended procedures 7.5-02-02-02, 2014
- Liu, W.T., Tang, W., Xie, X.: Wind power distribution over the ocean. *Geophysical research letters*, 35, 2008
- 515 Machado, C.F.R., De Medeiros, J-L., Araujo, O.F.Q., Alves, R.M.B.: A comparative analysis of methanol production routes: synthesis gas versus CO<sub>2</sub> hydrogenation. In Proc. of the 2014 International conference on industrial engineering and operations management, Bali, Indonesia, 2014
- Manwell, J.F., McGowan, J.G., Rogers, A.L.: *Wind energy explained: theory, design and application*. Wiley, 2009
- Marlin, D.S., Sarron, E., Sigurbjornsson, I.: Process advantages of direct CO<sub>2</sub> to methanol synthesis, *Frontiers in chemistry*,
- 520 6, 2018
- McDonagh S., O’Shea R., Wall D.M., Deane J.P., Murphy J.D.: Modelling of a power-to-gas system to predict the levelised cost of energy of an advanced renewable gaseous transport fuel. *Applied Energy*, 215, 444-456, 2018
- Meller M.: Wind-power linear motion hydrogen production systems. U.S. Patent 7,146,918 B2, 2006
- Morgan, E.R.: Techno-economic feasibility study of ammonia plants powered by offshore wind, *Dissertations* 697,
- 525 University of Massachussets – Amherst, 2013
- Norspower, Norspower rotor sails solution, Technical brochure, 2019
- Ouchi, K., Henzie, J.: Hydrogen generation sailing ship: conceptual design and feasibility study, In Proc. Of IEEE OCEANS 2017 conference, 2017
- Papanikolaou, A.: Chapter 2: Selection of main dimensions and calculation of basic ship design value. In: *Ship Design: methodologies of preliminary design*. Springer 628 pp., 2014
- 530 Pelz, P.F., Holl, M., Platzer, M.: Analytical method towards an optimal energetic and economical wind-energy converter. *Energy*, 94, 344-351, 2016

- Platzer, M.F., Sarigul-Klijn, N.: A novel approach to extract power from free-flowing water and high-altitude jet streams, In Proc. Of the ASME 2009 3rd International conference on energy sustainability Vol. 1, San Francisco, California, USA, 2009
- 535 Platzer, M.F., Lennie, M., Vogt, D.M.: Analysis of the conversion of ocean wind power into hydrogen, In Proc. Of the World Renewable Energy Conference, Perth, Australia, 2013
- Platzer, M.F., Sarigul-Klijn, N., Young, J., Ahsraf, M.A., Lai, J.C.S. :Renewable hydrogen production using sailing ships. Journal of energy resources technology, 136, 2014
- Platzer, M.F., Sarigul-Klijn, N.: Energy ships and plug-in electric vehicles: are they the key for a rapid transition to an emission-free economy? In Proc. Of the ASME 2015 International Mechanical Engineering Congress & Exposition (IMECE), Houston, Texas, USA, 2015
- 540 Salomon, R.E.: Process of converting wind energy to elemental hydrogen and apparatus therefor, U.S. Patent 4335093A, 1982
- Sanchez de Lara Garcia, J.P.: Wind turbine database: modelling and analysis with focus on upscaling. Masters thesis, Chalmers University of Technology, 2013
- 545 Schulz, L.: Private communication, 2019
- UNFCCC: Paris agreement, 2015
- Vazquez, F.V., Koponen, J., Russkanen, V., Bajamundi, C., Kosonen, A., Simell, P., Ahola, J., Frilund, C., Reinikainen, M., Heikkinen, N., Kauppinen, J., Piermartini, P.: Power-to-X technology using renewable electricity and carbon dioxide from ambient air: SOLETAIR proof-of-concept and improved process concept. Journal of CO2 utilization 28, 235-246, 2018
- 550 Vidal, J.P.: System for propulsion of boats by means of winds and streams and for recovery of energy, US Patent 4,371,346, 1983